Agricultural Water Management 235 (2020) 106153

Contents lists available at ScienceDirect

Agricultural Water Management

journal homepage: www.elsevier.com/locate/agwat

Root morphological characteristics and soil water infiltration capacity in semi-arid artificial grassland soils

Yu Liu[a,b], Lei Guo[a], Ze Huang[a], Manuel López-Vicente[c], Gao-Lin Wu[a,b,d,*]

[a] State Key Laboratory of Soil Erosion and Dryland Farming on the Loess Plateau, Northwest A & F University, Yangling, Shaanxi, 712100, China
[b] Institute of Soil and Water Conservation, Institute of Soil and Water Conservation, Chinese Academy of Sciences and Ministry of Water Resource, Yangling, Shaanxi, 712100, China
[c] Team Soil, Water and Land Use, Wageningen Environmental Research, Droevendaalsesteeg 3, Wageningen, 6708RC, Netherlands
[d] CAS Center for Excellence in Quaternary Science and Global Change, Xi'an, 710061, China

ARTICLE INFO

Keywords:
Root morphological characteristics
Soil infiltration rate
Double-ring infiltrometer
Artificial grassland
Semi-arid area

ABSTRACT

Surface water infiltration is an important process to meet plant water needs and an important part of the hydrological cycle via groundwater recharge, with special relevance in semi-arid regions. This study evaluated the relationships between grassland plant root morphological characteristics and soil water infiltration rates (IR: initial, steady and average). For this purpose, five artificial homogeneous grasslands (*Melilotus suaveolens*, *Medicago sativa*, *Panicum virgatum*, *Bromus inermis* and *Miscanthus sinensis*) without irrigation or fertilization were studied in the Loess Plateau. The observed steady IR were significantly different between the 1-year grasslands: *M. suaveolens* > *M. sativa* > *P. virgatum* > *B. inermis* > *M. sinensis*. The root length density and root surface area were negatively correlated with the average, initial and steady IR at different soil depths ($p < 0.05$). However, the root volume did not significantly influence IR. The stepwise multiple regression determined that the main factors controlling IR were the root length density at the depth of 5 − 30 cm and root surface area at the depth of 10 − 20 cm. Our results provide insight into the influence of grassland root morphological characteristics on water infiltration in drylands and are of interest for soil water supply programs in forage production.

1. Introduction

Soil moisture is the main limiting factor for the development of agriculture production and ecological restoration in arid and semi-arid regions (Khan et al., 2009). Excessive planting of non-native species increases soil water deficit, which in turn impedes the sustainable development of vegetation in arid and semi-arid regions (Liu et al., 2018; López-Vicente and Álvarez, 2018; Jia et al., 2019). Thus, it is essential for ecological recovery to maximize the retention of precipitation and reduce runoff in these areas (Shi and Shao, 1999). In order to address this issue, a series of re-vegetation projects have been implemented by the Chinese Government to mitigate soil and water loss and restore the ecological environment in arid and semi-arid regions.

Grassland is one of the main types of vegetation for restoration in arid and semi-arid regions. Previous studies have shown that compared to forest, grasslands can maintain soil moisture better and achieve the sustainable vegetation restoration (Huang et al., 2017). Their dense root system contributes to plant survival in extreme climatic conditions and improves the surface soil properties (Shi et al., 2012; Wu et al., 2014). The intertwined disturbance of root systems and the loose and penetrating effect of vegetation on soil were brought into full play to improve soil structure. Grass roots have a significant effect on water storage and soil infiltration capacity (Jotisankasa and Sirirattanachat, 2017). The formation of continuous open macropores after root death and decay is of great significance to accelerate soil water migration and improve soil permeability in alfalfa grassland (Guo et al., 2019). Consequently, the role of grassland in increasing infiltration and decreasing runoff has been paid great attention in many arid and semi-arid regions (Wu et al., 2016, 2017).

Root-dominated underground hydrological processes at the root-soil interface plays an important role in the water cycle of grassland ecosystems (Volpe et al., 2013). Previous studies have focused on the preferential flow resulted from plant roots biomass (Ceccon et al., 2011; Zhao et al., 2016). Plant roots could not only form continuous macropores or preferential root channels, but also form rigid pores larger than their diameters, which can affect the movement and connectivity of

* Corresponding author at: State Key Laboratory of Soil Erosion and Dryland Farming on the Loess Plateau, Northwest A & F University, NO. 26 Xinong Road, Yangling, Shaanxi Province, 712100, People's Republic of China.
E-mail address: wugaolin@nwsuaf.edu.cn (G.-L. Wu).

https://doi.org/10.1016/j.agwat.2020.106153
Received 28 January 2020; Received in revised form 14 March 2020; Accepted 16 March 2020
Available online 21 March 2020
0378-3774/

water and solutes (Tracy et al., 2011; Huang et al., 2017). Both living and decaying roots contribute to soil infiltration by increasing macropores and soil aggregation (Benegas et al., 2014). Besides, root residues are the main carbon input of soil and the important source of soil organic matter in grassland ecosystem. Humus and polysaccharides in organic matter are the most important cementing medium for the formation of water-stabilized aggregates, which can promote the formation of soil aggregate structure. As a result of these processes, the soil with well-developed aggregate structure has high porosity and water retention, which plays an important role in increasing soil water storage capacity (Six et al., 2004).

The morphological structure of root directly determines the spatial distribution of root channel, which is closely related to the infiltration of soil water (Fan et al., 2017; Cui et al., 2019). The difference of root morphology and structure of different types of grassland leads to the separation of niche in the utilization of soil water resources, and thus, it affects the infiltration process of soil water (Leung et al., 2015; Wu et al., 2017). Namely, legume grassland promotes water infiltration better than gramineous grassland in semi-arid regions (Huang et al., 2017). Fibrous roots of gramineous grass are mainly concentrated in the surface soil (0 − 30 cm) forming a dense network to influence water movement (Archer et al., 2002; Ng et al., 2016; Liu et al., 2019). Furthermore, fine roots could increase soil organic matter and form soil pores determining the potential of soil infiltration in semi-arid regions (Cui et al., 2019). The roots of legume grass are characterized by a large-diameter, long almost-straight taproot, which can reach a depth of a few meters in semi-arid areas (Guo et al., 2019). Deep-rooted plants can effectively increase the root depth and subsoil water storage capacity (Cerdà et al., 2009; Leung et al., 2015). Therefore, legume grassland promotes precipitation infiltration better than gramineous grassland in semi-arid areas (Huang et al., 2017). Macropores or channels created by plant root systems are important paths for downward movement of water in arid and semi-arid regions. Previous studies have mainly focused on the effects of root system on the soil properties or characterized root characteristics by biomass determining whole water infiltration process. However, the root cause of these results, the morphological characteristics of the root system were weakened. The relationship between root morphological characteristics and water infiltration process are poorly understand. This is essential for better understanding of water infiltration and soil moisture conservation in semi-arid grassland ecosystems.

In this study, we measured the plant roots morphological characteristics (i.e., root length density, root surface area and root volume) at five typical artificial grasslands (*Melilotus suaveolens*, *Medicago sativa*, *Panicum virgatum*, *Bromus inermis* and *Miscanthus sinensis*) under natural conditions to determine their effects on water infiltration process in a semi-arid area. The specific objectives of this study were to: (1) evaluate the relative role played by different plant root morphological characteristics on infiltration rates; and (2) identify the key soil and root morphological parameters that mainly control the infiltration rate at different infiltration stages. The results can provide the opportunity to clarify the relative importance of root morphological characteristics during infiltration process, and further contribute with new insights into soil water infiltration for vegetation restoration.

2. Materials and methods

2.1. Study area

The study was conducted in the Xiaqu town of Wenshui County of Lvliang city in Shanxi Province, China (111°29′-112°19′E, 37°15′-37°35′N). The area is a part of the typical yellow landform located in the eastern part of the Loess Plateau (in the east of central China). The study site has an elevation ranging from 739 m to 2169 m above the mean sea level. The climate is temperate semi-arid continental with a mean annual precipitation of 457 mm. Although precipitation is interannually uneven, most of the average annual rainfall depth, ca. 60 %, was recorded between June and August. The main climatic characteristics in this area are an average annual temperature of 10.01 °C and the marked differences between the extreme maximum (39.9 °C) and minimum (-30.5 °C) temperatures. The sunshine duration is 2351.7–2871.7 h and the frost-free period lasts 133–178 days. The soil type is mainly Loessial and Castanozems.

2.2. Experimental treatment

Five typical artificial grasslands were established in this study: *Melilotus suaveolens, Medicago sativa, Panicum virgatum, Bromus inermis and Miscanthus sinensis*. All forage plants were planted in 2017 and three replicate plots (6 m × 6 m) were constructed on each grassland type. After plantation, forage growth completely depended on rainfall, without additional fertilizations, human interventions or animal disturbances. This treatment ensured that the conditions in all the plots were similar, and thus, any differences were entirely due to the grassland type. All experimental processes were conducted in September 2018.

The soil infiltration rates were determined by using the double-ring infiltrometer. Nine replicates were performed for each grassland type. At each site, a flat land was selected for doing the infiltrating experiment. Later on, all plants were cut off at ground level and the litter layer was carefully removed. Then, the PVC pipes, which were of 16-cm inner diameter, 32-cm outer diameter and 20-cm height, were placed concentrically on the soil surface. The pipes were gently inserted about 10 cm deep into the soil using a rubber hammer while ensuring that the rings were levelled during the insertion. The soil placed outside the PVC pipes was compacted to avoid water leaving out of the PVC pipes. After that, water was added into the inner and outer rings respectively until the water depth reached 5 cm at the same time. Afterwards, the time required for the water level to drop 0.5 cm in the inner ring was recorded with a stopwatch until three consecutive measured infiltration times remained unchanged, and the infiltration rate was considered to be at steady state. The water levels of the inner and outer rings were consistent during the infiltration process. To calculate the initial infiltration rate (IIR), only the first three minutes of the infiltration process were taken into consideration. The average of the last three fairly constant infiltration rates was considered as the steady-state infiltration rate (SIR). These rates were calculated following the equation of Zhang et al. (2017):

$$i = \Delta I / \Delta t \times 600 \quad (1)$$

where i is the infiltration rate (mm h^{-1}), ΔI is the cumulative infiltration in the inner ring (cm) during Δt time of infiltration (min), and 600 is a unit conversion factor.

2.3. Soil sampling and analysis

In each plot, soil samples were collected at the same soil depth intervals of 0 − 10 cm, 10 − 20 cm, 20 − 30 cm, 30 − 40 cm and 40 − 50 cm, and three replicates were conducted for each soil layer. The gravimetric soil water content (SWC, %) was measured by taking the proportion of the loss of mass, after oven-drying at 105 °C, to the constant mass of dry soil. The soil bulk density (BD, g cm^{-3}) was measured using a stainless-steel cylindrical ring of 100 cm^3 volume to collect the samples. The total soil porosity (TP, %) was calculated with the formula:

$$TP = (1 - BD/ds) \times 100 \quad (2)$$

where ds is the particle density (g cm^{-3}), which was assumed to be 2.65 g cm^{-3}. The mean and standard error values of the soil physical properties are shown in Table 1.

Table 1
Mean ± standard error values of the soil physical properties (SWC, soil water content by mass; BD, soil bulk density; TP, total soil porosity) at the depth of 0-50 cm in the different artificial grasslands.

Grassland type	Soil depth (cm)	SWC (%)	BD (g cm^{-3})	TP (%)
M. suaveolens	0-10	10.07 ± 0.41b	1.22 ± 0.06a	53.83 ± 2.38a
	10–20	11.46 ± 0.64a	1.39 ± 0.03a	47.42 ± 1.28a
	20-30	9.16 ± 0.75b	1.42 ± 0.01b	46.40 ± 0.32a
	30–40	7.46 ± 0.41b	1.38 ± 0.04bc	47.71 ± 1.39abc
	40–50	8.89 ± 0.35b	1.39 ± 0.03a	47.38 ± 1.23b
M. sativa	0-10	9.63 ± 0.98b	1.27 ± 0.04a	52.18 ± 1.42a
	10–20	10.08 ± 0.58a	1.33 ± 0.01b	49.75 ± 0.43a
	20-30	12.11 ± 0.64a	1.49 ± 0.03a	43.74 ± 1.28b
	30–40	11.46 ± 3.12b	1.38 ± 0.03abc	47.95 ± 1.09ab
	40–50	7.41 ± 0.23b	1.39 ± 0.02a	47.52 ± 0.73b
P. virgatum	0-10	13.11 ± 0.71a	1.33 ± 0.05a	49.91 ± 2.06a
	10–20	12.04 ± 0.46a	1.39 ± 0.06a	47.64 ± 2.11a
	20-30	12.78 ± 3.60a	1.41 ± 0.01b	46.77 ± 0.32a
	30–40	15.70 ± 1.54a	1.31 ± 0.05c	50.75 ± 1.95a
	40–50	13.21 ± 0.60a	1.28 ± 0.04b	51.52 ± 1.46a
B. inermis	0-10	8.09 ± 0.93b	1.28 ± 0.03a	51.59 ± 1.24a
	10–20	10.32 ± 1.82a	1.39 ± 0.03a	47.43 ± 1.33a
	20-30	10.37 ± 0.70b	1.49 ± 0.01a	43.59 ± 0.40b
	30–40	7.13 ± 0.44b	1.41 ± 0.02ab	46.71 ± 0.78bc
	40–50	8.53 ± 0.22b	1.36 ± 0.02a	48.52 ± 0.72b
M. sinensis	0-10	13.29 ± 1.49a	1.28 ± 0.08a	51.84 ± 3.06a
	10–20	11.83 ± 0.81a	1.40 ± 0.02a	47.17 ± 0.70a
	20-30	11.42 ± 0.55a	1.51 ± 0.00a	42.97 ± 0.04b
	30–40	14.36 ± 2.70a	1.48 ± 0.03a	44.28 ± 1.03c
	40–50	14.50 ± 0.60a	1.39 ± 0.01a	47.39 ± 0.28b

Note: For each soil depth but different artificial grassland, the values followed by a different letter are significantly different at 0.05 level.

2.4. Plant root sampling

The vertical soil profiles were excavated at each experimental plot 24 h after finishing the infiltration experiment. Two soil samples were taken to determine the plant roots distribution in the soil profile with 0.2 m × 0.2 m quadrats at each soil depth. Samples were taken at six intervals up to a depth of 50 cm (0–5, 5–10, 10–20, 20–30, 30–40 and 40 – 50 cm) in each plot. The roots were separated from soil sample by using a 5 mm mesh sieve, and then, the roots were placed in basins with water to be gently washed so that the soil particles and debris could be removed. The roots were scanned and analyzed using the WinRHIZO root analysis system for morphological parameter measurements. The root length density (RLD) – defined as the total root length per soil volume (mm $(100\ cm^3)^{-1}$), root surface area (RSA; cm^2) and root volume (RV; cm^3) were estimated.

2.5. Statistical analysis

All data were expressed as mean value ± standard error and the statistical analyses were performed using SPSS 22.0 software. One-way analysis of variance (ANOVA) and the least significance difference (LSD) post hoc test were used to analyze the differences of soil properties and the differences in the initial (IIR), steady (SIR) and average (AIR) infiltration rates among the different grasslands. The differences in RLD, RSA and RV among the different grasslands and soil depth intervals were assessed by using the same statistic analysis. The Pearson correlation coefficient was used to express the correlation between the infiltration rates and root parameters. The main influence factors of root morphological characteristics on soil infiltration rate were determined by stepwise multiple regression. All significant differences were evaluated at 0.05 level.

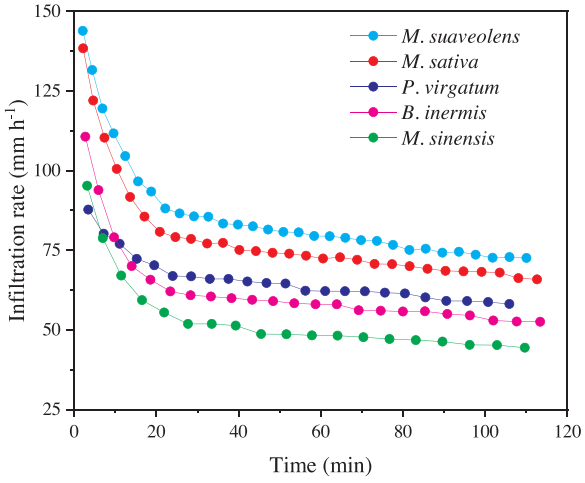

Fig. 1. Soil infiltration rates in the different artificial grasslands.

3. Results

3.1. Soil water infiltration in the different grasslands

The infiltration rates decreased significantly at the initial stage and then gradually tended to be stable (Fig. 1). The SIR in the *M. suaveolens* (72.70 ± 0.15 mm h^{-1}) grassland showed significant differences with those values in *M. sativa* (66.69 ± 1.12 mm h^{-1}), *P. virgatum* (58.65 ± 0.47 mm h^{-1}), *B. inermis* (52.69 ± 0.21 mm h^{-1}) and *M. sinensis* (44.98 ± 0.49 mm h^{-1}) grasslands ($p < 0.05$) (Table 2). Regarding the IIR, the highest values were observed in the *M. suaveolens* grassland (143.86 ± 15.92 mm h^{-1}), followed by *M. sativa* (138.37 ± 13.54 mm h^{-1}), *B. inermis* (110.65 ± 11.68 mm h^{-1}) and *M. sinensis* (95.24 ± 8.75 mm h^{-1}), while the IIR in *P. virgatum* (87.75 ± 10.83 mm h^{-1}) was significantly lower than in the other four grasslands (Table 2). The AIR in the *M. sinensis* grassland was significantly lower than in the other four grasslands ($p < 0.05$) (Table 2).

3.2. Root distribution and root morphological characteristics

The roots distribution in the soil was shown in Fig. 2. The changes in the root length density (RLD), root surface area (RSA) and root volume (RV) with increasing the soil depth depicted similar trends (from higher to lower values) in the three parameters and were similar among the different grasslands (Fig. 3). The largest RLD, RSA and RV were recorded in the upper soil layers (0 – 20 cm) and the lowest in the subsoil. Regarding the magnitude of the parameters, the RLD, RSA and RV were different in the distinct grassland types. In terms of root length density (RLD), the values of *M. sinensis* were significantly higher than those observed in the other artificial grasslands ($p < 0.05$). With respect to the root surface area (RSA), the *M. sinensis*, *B. inermis* and *P. virgatum* grasslands had higher values than those measured in the *M. sativa* and *M. suaveolens* grasslands. Regarding to root volume (RV), the values of

Table 2
Soil water infiltration rates (mean ± SD) in the different artificial grasslands.

Grassland type	IIR (mm h^{-1})	SIR (mm h^{-1})	AIR (mm h^{-1})
M. suaveolens	143.86 ± 15.92a	72.70 ± 0.15a	87.10 ± 10.66a
M. sativa	138.37 ± 13.54a	66.69 ± 1.12b	79.84 ± 8.51a
P. virgatum	87.75 ± 10.83b	58.65 ± 0.47c	65.86 ± 7.52a
B. inermis	110.65 ± 11.68a	52.69 ± 0.21d	62.91 ± 6.48a
M. sinensis	95.24 ± 8.75a	44.98 ± 0.49e	54.09 ± 6.08b

Note: IIR, the initial infiltration rate; SIR, the steady infiltration rate; AIR, the average infiltration rate. Values followed by a different letter in the same column were significantly different at the 0.05 level (LSD).

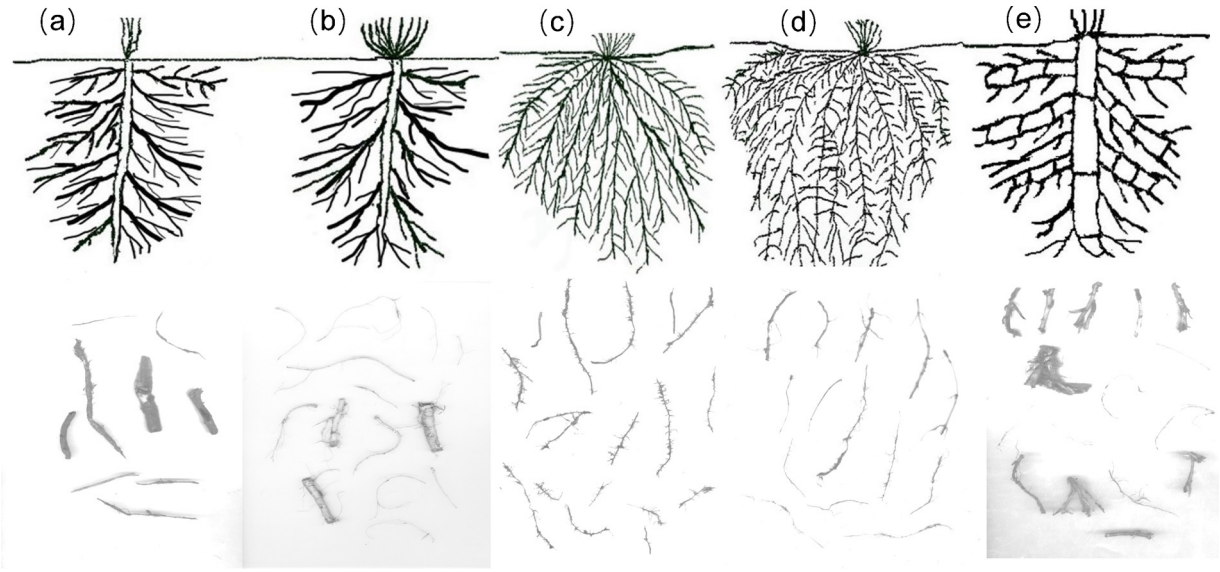

Fig. 2. The distribution of plant roots systems (above) and the real images of root at the depth of 0-5 cm (below) in different artificial grasslands. Note: (a): *M. suaveolens*; (b): *M. sativa*; (c): *P. virgatum*; (d): *B. inermis*; (e): *M. sinensis*.

M. sinensis, *P. virgatum* and *M. sativa* were significantly higher than those of *B. inermis* and *M. suaveolens* at the soil depth of 0 – 20 cm ($p < 0.05$).

3.3. Correlation between root morphological characteristics and infiltration rates

The correlation analyses showed that the AIR had highly significant negative correlation with RLD and RSA at depth of 0 – 50 cm ($p < 0.01$) (Table 3). The IIR had highly significant negative relationship with the RLD at the depth of 0 – 40 cm and with the RSA at the depth of 0–5 and 20 – 40 cm ($p < 0.01$). The SIR was significantly and negatively related to the RLD at depth of 0 – 40 cm ($p < 0.01$). Moreover, the SIR was significantly and negatively related to the RSA at the depth of 20 – 50 cm ($p < 0.05$) (Table 3). The statistical analysis with multiple-regression highlighted that the main root factors that affected soil infiltration rates were the RLD at the soil intervals of 5 – 10 cm (RLD10), 10 – 20 cm (RLD20), and 20 – 30 cm (RLD30), and the RSA at the soil interval of 10 – 20 cm (RSA20, Table 4). The RLD20 and RLD30 were thought to be the negative main influencing factors of AIR. Similarly, the RLD30 was the most important factor for the IIR. The RLD10, RLD30 and RSA20 were negative factors for SIR.

4. Discussion

Root systems determine the spatial distribution of root channel, which is closely related to water infiltration in soil. This process is essential for soil water recharge and vegetation maintenance in semi-arid areas. Our results found that plant roots density and complexity decreased along the soil depth. The largest root length density, root surface area and root volume were recorded at the depth of 0 – 20 cm soil. These results can be partially explained by the age of the grasslands' plantation, younger than 2 years at the time of the field survey. Plant roots near the surface soil can improve the physical and chemical properties of the soil, such as the soil bulk density, porosity and soil organic matter (Leung et al., 2015). Plant roots also improve soil infiltration capacity by increasing soil porosity and organic matter in topsoil (Alaoui et al., 2015; Huang et al., 2017). In addition, during plant root decomposition, plant roots in the upper layer of the soil form more preferential root channels than those in the subsoil (Jørgensen et al., 2002). Our results are in accordance with these studies and prove that the distribution of roots in the different soil layers are significantly related to water infiltration, which depends on the morphological characteristics of root systems.

Root morphological characteristics are important indicators of plant root growth due to their role in regulating the water and nutrient cycles

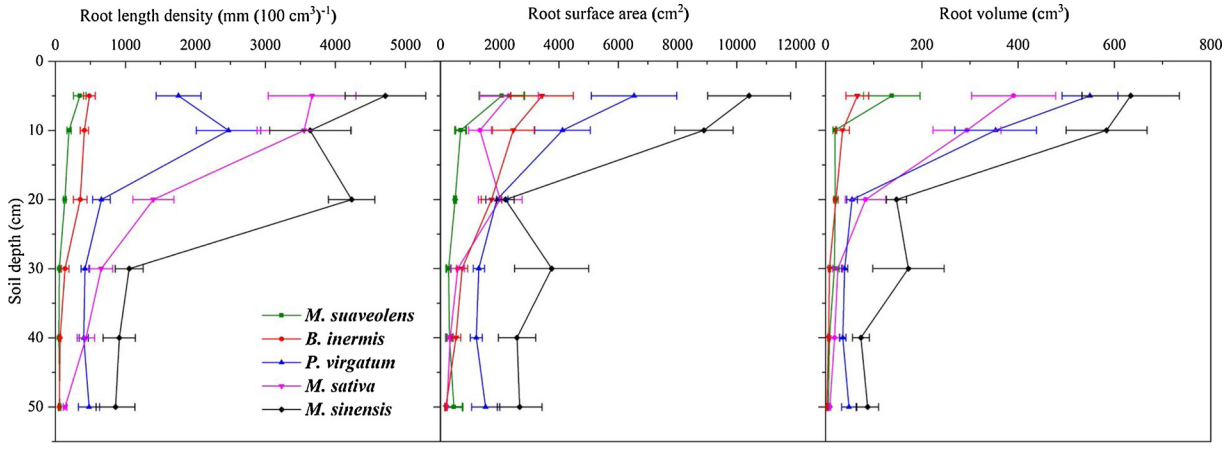

Fig. 3. Changes in root characteristics between the different artificial grasslands. The relationship between root characteristics and soil depth was illustrated.

Table 3
Matrix showing correlations (correlation coefficient) between plant root characteristics and infiltration rates of AIR, IIR and SIR.

Items	RLD5	RLD10	RLD20	RLD30	RLD40	RLD50
AIR	−0.364*	−0.335*	−0.537**	−0.615**	−0.510**	−0.303*
IIR	−0.336*	−0.308*	−0.432**	−0.558**	−0.411**	−0.285
SIR	−0.337*	−0.313*	−0.568**	−0.594**	−0.498**	−0.292
Items	RSA5	RSA10	RSA20	RSA30	RSA40	RSA50
AIR	−0.303*	−0.301*	−0.468**	−0.437**	−0.420**	−0.369*
IIR	−0.311*	−0.264	−0.338*	−0.324*	−0.331*	−0.271
SIR	−0.252	−0.273	−0.501**	−0.437**	−0.387**	−0.375*
Items	RV5	RV10	RV20	RV30	RV40	RV50
AIR	−0.135	0.281	−0.213	−0.300	0.031	−0.109
IIR	−0.152	0.332	−0.044	−0.189	0.123	−0.025
SIR	−0.107	0.128	−0.238	−0.314	0.011	−0.111

Note: AIR, the average infiltration rate; IIR, the initial infiltration rate; SIR, the steady infiltration rate; RLD5, 10, 20, 30, 40 and 50, root length density at the depths of 0 − 50 cm; RSA5, 10, 20, 30, 40 and 50, root surface area at the depths of 0 − 50 cm; RV5, 10, 20, 30, 40 and 50, root volume at the depths of 0 − 50 cm. * Correlation is significant at the $p < 0.05$ probability level (2-tailed), ** Correlation is significant at the $p < 0.01$ probability level (2-tailed), respectively.

Table 4
Multiple-regression equations between infiltration rates (AIR, IIR and SIR) and root characteristics.

	Regression equation	R^2
AIR	Y1 = 62.287 - 0.004RLD20 - 0.014RLD30	0.615
IIR	Y2 = 79.207 - 0.028RLD30	0.558
SIR	Y3 = 149.455 - 0.015RLD10 - 0.014RLD30 - 0.002RSA20	0.665

Note: AIR, the average infiltration rate; IIR, the initial infiltration rate; SIR, the steady infiltration rate; RLD10, 20 and 30, root length density at the depths of 5–10, 10–20 and 20 − 30 cm; RSA20, root surface area at the depths of 10 − 20 cm.

required for plant growth. The root length density can reflect the extent of the distribution, interpenetration and interweaving of the root system in the soil, affecting the soil water migration. Li et al. (2013) demonstrated that water flow paths appear between the root system surface and the soil contact surface, forming biological macropores, which have an important influence during the different stages of soil water infiltration. This complex system plays a significant role in soil water uptake and nutrient transfer. The results of this study showed that the grasslands root morphological characteristics had significant effects on soil infiltration at various infiltration stages. A smaller RLD, RSA and RV increased water infiltration. Multiple channels formed by fine roots could form preferential flow during infiltration, but this promotion decreased with the increase of RLD. This effect can be explained by the abundant root network that could clog the soil pore space, and thus, favored a decrease in the soil infiltration rates, such as Cui et al. (2019) observed in grasslands. With the increase of RLD, the squeezing effect of strong root systems on soil caused higher values of soil bulk density and lower of soil porosity, which jointly provoked a decrease of water infiltration. There is another context to bear in mind too, because plant roots can enmesh and realign soil particles and release exudates resulting in changes in soil properties, which in turn affect the soil infiltration capacity (Bronick and Lal, 2005).

Plant roots can result in changes in the size distribution and connectivity of soil pores that affect the water infiltration processes. Root morphological characteristics integrate both chemical and physical properties associated with root development. Moreover, these parameters also reflect basic soil conditions for water infiltration. Sanders et al. (2012) proved that plant roots develop into macropores and generate macropores (biopores, cracks and burrows) during the process of plant root growth. The formation of macropores or blocking or squeezing pores in the soil is closely related to the root morphological characteristics (Archer et al., 2002; Cui et al., 2019). Another consideration is that fine plant roots begin to decay at a higher rate because the growth cycle of fine plant roots is short, ranging from a few months to several years. The longevity of fine plant roots is related to the process of fine plant roots regeneration in which the new roots replace the decayed roots (Yavitt et al., 2011). Meanwhile, preferential root channel is formed during root decomposition. There processes mainly take place in the topsoil where most plant roots are distributed. Our results also showed that the characteristics of surface root system were significantly correlated with the initial, steady and average infiltration rates. Compared with living roots, decayed roots would more effectively create preferential root channels, such as Zhang and Wang (2015) observed in middle latitude areas where fine roots decomposed significantly faster than coarse roots.

Given the importance of plant roots in soil water uptake, this study offers relevant data about how plant root characteristics of different grassland types affect soil water infiltration. The statistical analysis of our field observations – without human disturbances during plant growth – allowed to conclude that the main root factors clearly affecting the soil infiltration rates were RLD10, RLD20, RLD30 and RSA20. Previous studies reported that the infiltration capacity of different species was different because of the different root characteristics (i.e., root diameter and root distribution) (Leung et al., 2017; Cui et al., 2019). Our findings showed that the different soil infiltration rates (AIR, IIR and SIR) were negatively correlated with the root length density and root surface area, but not with the root volume. This discrepancy could be explained by the presence of certain plant functional groups, such as grasses forage (*B.inermis*) and legumes forage (*M. sativa*) that had a significant impact on soil infiltration (Wu et al., 2014). Christine et al. (2014) also found that soil infiltration rates were increased by legumes forage and decreased by grasses forage. In addition, the soil infiltration rates were higher under *M. sativa* and *M. suaveolens* grasslands than under *M. sinensis* grassland. However, the values of RLD and RSA of *M. sativa* and *M. suaveolens* grasslands were smaller than those values measured in the *M. sinensis* grassland. This fact may be attributed to the *M. sinensis* (grass forage) grassland characteristics that have many coarse and rhizomatous roots, which tend to compact the soil and block the water flow, and thus, decrease soil infiltration rate (Cui et al., 2019). In general, gramineous forage with fibrous and rhizomatous roots grows densely near the surface soil to form a dense network that blocks the soil pore space, reduces water movement and decreases soil infiltration rate (Archer et al., 2002); while legume forage with tap roots would increase water infiltration into the soil.

5. Conclusions

Plant root morphological characteristics significantly affected the soil surface-water infiltration capacity despite the inherent differences in the root characteristics of the five different artificial grasslands evaluated in this study under semi-arid natural conditions. The soil infiltration capacity of the artificial grasslands was significantly different between them: *M. suaveolens* > *M. sativa* > *P. virgatum* > *B. inermis* > *M. sinensis*. The density and complexity of the plant root systems decreased with soil depth and roots were mainly distributed near the surface soil up to a depth of 20 cm for the different grasslands. The root length density and root surface area were negatively correlated with the infiltration rates, while the root volume was not significantly correlated with the infiltration rates. The root length density at 5 − 10 cm, 10 − 20 cm and 20 − 30 cm depth and the root surface area at 10 − 20 cm depth were the main factors that had a clear influence on the soil water infiltration rates at the initial, steady-state and average stages. These results contribute to interpret the influence of plant root morphological characteristics on the infiltration processes in dryland

forage production and to improve the understanding of the effect of plant roots on soil water supply in dryland agriculture production in water-scarce areas. Further study is necessary to demonstrate the relationships between root characteristics and infiltration response in arid areas where water scarcity is common and plants are subjected to more serious water stress than in semiarid areas.

Declaration of interests

The authors declare that they have no known competing financial interests or personal relationships that could have appeared to influence the work reported in this paper.

Acknowledgements

This research was funded by the Projects of the National Natural Science Foundation of ChinaNSFC 41977063, 41722107, the Key Technologies Research and Development Program of Shaanxi Province 2017NY-065, the Light of West China Program of the Chinese Academy of Sciences (XAB2015A04; XAB2018B09).

References

Archer, N.A.L., Quinton, J.N., Hess, T.M., 2002. Below-ground relationships of soil texture, roots and hydraulic conductivity in two-phase mosaic vegetation in south-east Spain. J. Arid Environ. 52, 535–553.

Benegas, L., Ilstedt, U., Roupsard, O., Jones, J., Malmer, A., 2014. Effects of trees on infiltrability and preferential flow in two contrasting agroecosystems in central America. Agr. Ecosyst. Environ. 183, 185–196.

Bronick, C.J., Lal, R., 2005. Soil structure and management: a review. Geoderma 124, 3–22.

Ceccon, C., Panzacchi, P., Scandellari, F., Prandi, L., Ventura, M., Russo, B., Millard, P., Tagliavini, M., 2011. Spatial and temporal effects of soil temperature and moisture and the relation to fine root density on root and soil respiration in a mature apple orchard. Plant Soil 342, 195–206.

Cerdà, A., Juergensen, M.F., Bodí, M.B., 2009. Effects of ants on water and soil losses from organically-managed citrus orchards in Eastern Spain. Biologia 64, 527–531.

Christine, F., Christiane, R., Britta, J., Nico, E., Jussi, B., Sabine, A., Stefan, S., Wolfgang, W.W., Jens, S., Anke, H., 2014. How do earthworms, soil texture and plant composition affect infiltration along an experimental plant diversity gradient in grassland. PLoS One 9, e98987.

Cui, Z., Wu, G.L., Huang, Z., Liu, Y., 2019. Fine roots determine soil infiltration potential than soil water content in semi-arid grassland soils. J. Hydrol. 578, 124023.

Fan, Y., Miguezmacho, G., Jobbágy, E.G., Jackson, R.B., Oterocasal, C., 2017. Hydrologic regulation of plant rooting depth. Proc. Natl. Acad. Sci. U. S. A. 114, 10572–10577.

Guo, L., Liu, Y., Wu, G.L., Huang, Z., Cheng, Z., Zhang, R.Q., Tian, F.P., He, H., 2019. Preferential water flow: influence of alfalfa (*Medicago sativa* L.) decayed root channels on soil water infiltration. J. Hydrol. 578, 124019.

Huang, Z., Tian, F.P., Wu, G.L., Liu, Y., Dang, Z.Q., 2017. Legume grasslands promote precipitation infiltration better than gramineous grasslands in arid regions. Land Degrad. Dev. 28, 309–316.

Jia, X.X., Shao, M.A., Yu, D.X., Zhang, Y., Binley, A., 2019. Spatial variations in soil-water carrying capacity of three typical revegetation species on the Loess Plateau, China. Agr. Ecosyst. Environ. 273, 25–35.

Jørgensen, P.R., Hoffmann, M., Kistrup, J.P., Bryde, C., Bossi, R., Villholth, K.G., 2002. Preferential flow and pesticide transport in a clay-rich till: field, laboratory, and modeling analysis. Water Resour. Res. 38, 1246–1261.

Jotisankasa, A., Sirirattanachat, M.T., 2017. Effects of grass roots on soil-water retention curve and permeability. Can. Geotech. J. 54, 1612–1622.

Khan, S., Hanjra, M.A., Mu, J.X., 2009. Water management and crop production for food security in China: a review. Agr. Water Manage. 96, 349–360.

Leung, A.K., Garg, A., Coo, J.L., Ng, C.W.W., Hau, B.C.H., 2015. Effects of the roots of *Cynodon dactylon* and *Schefflera heptaphylla* on water infiltration rate and soil hydraulic conductivity. Hydrol. Proc. 29, 3342–3354.

Leung, A.K., Boldrin, D., Liang, T., Wu, Z.Y., Kamchoom, V., Bengough, A.G., 2017. Plant age effects on soil infiltration rate during early plant establishment. Gotechnique 68, 646–652.

Li, J.X., He, B.H., Chen, Y., 2013. Root features of typical herb plants for hillslope protection and their effects on soil infiltration. Acta Ecol. Sin. 33, 1535–1547.

Liu, Y., Miao, H.T., Huang, Z., Cui, Z., He, H., Zheng, J., Han, F., Chang, X., Wu, G.L., 2018. Soil water depletion patterns of artificial forest species and ages on the Loess Plateau (China). Forest Ecol. Manage. 417, 137–143.

Liu, Y., Cui, Z., Huang, Z., López-Vicente, M., Wu, G.L., 2019. Influence of soil moisture and plant roots on the soil infiltration capacity at different stages in arid grasslands of China. Catena 182, 104147.

López-Vicente, M., Álvarez, S., 2018. Stability and patterns of topsoil water content in rainfed vineyards, olive groves, and cereal fields under different soil and tillage conditions. Agr. Water Manage. 201, 167–176.

Ng, C.W.W., Ni, J.J., Leung, A.K., Wang, Z.J., 2016. A new and simple water retention model for root-permeated soils. Géotech. Lett. 6, 106–111.

Sanders, E.C., Abou Najm, M.R., Mohtar, R.H., Kladivko, E., Schulze, D., 2012. Field method for separating the contribution of surface-connected preferential flow pathways from flow through the soil matrix. Water Resour. Res. 48, 4534–4542.

Shi, H., Shao, M.A., 1999. Soil and water loss from the Loess Plateau in China. J. Arid Environ. 45, 9–20.

Shi, Z.H., Fang, N.F., Wu, F.Z., Wang, L., Yue, B.J., Wu, G.L., 2012. Soil erosion processes and sediment sorting associated with transport mechanisms on steep slopes. J. Hydrol. (Amst) 454-455, 123–130.

Six, J., Bossuyt, H., Degryze, S., Denef, K., 2004. A history of research on the link between (micro) aggregates, soil biota, and soil organic matter dynamics. Soil Till. Res. 79, 7–31.

Tracy, S.R., Black, C.R., Roberts, J.A., Mooney, S.J., 2011. Soil compaction: a review of past and present techniques for investigating effects on root growth. J. Environ. Sci. Health B 91, 1528–1537.

Volpe, V., Marani, M., Albertson, J.D., Katul, G., 2013. Root controls on water redistribution and carbon uptake in the soil-plant system under current and future climate. Adv. Water Resour. Prot. 60, 110–120.

Wu, G.L., Zhang, Z.N., Wang, D., Shi, Z.H., Zhu, Y.J., 2014. Interactions of soil water content heterogeneity and species diversity patterns in semi-arid steppes on the Loess Plateau of China. J. Hydrol. 519, 1362–1367.

Wu, G.L., Yang, Z., Cui, Z., Liu, Y., Fang, N.F., Shi, Z.H., 2016. Mixed artificial grasslands with more roots improved mine soil infiltration capacity. J. Hydrol. 535, 54–60.

Wu, G.L., Liu, Y., Yang, Z., Cui, Z., Deng, L., Chang, X.F., Shi, Z.H., 2017. Root channels to indicate the increase in soil matrix water infiltration capacity of arid reclaimed mine soils. J. Hydrol. 546, 133–139.

Yavitt, J.B., Harms, K.E., Garcia, M.N., Mirabello, M.J., Wright, S.J., 2011. Soil fertility and fine root dynamics in response to 4 years of nutrient (N, P, K) fertilization in a lowland tropical moist forest, Panama. Aust. Ecol. 36, 433–445.

Zhang, X.Y., Wang, W., 2015. The decomposition of fine and coarse roots: their global patterns and controlling factors. Sci. Rep. 5, 9940.

Zhang, J., Lei, T.W., Qu, L.Q., Chen, P., Gao, X.F., Chen, C., Yuan, L.L., Zhang, M.L., Su, G.X., 2017. Method to measure soil matrix infiltration in forest soil. J. Hydrol. 552, 241–248.

Zhao, C., Gao, J., Huang, Y., Wang, G., Zhang, M., 2016. Effects of vegetation stems on hydraulics of overland flow under varying water discharges. Land Degrad. Dev. 27, 748–757.